

A simple framework to calibrate a soil water balance model with Sentinel-1 and Sentinel-2 observations over irrigated fields

Martina Natali
CIMA Research Foundation,
Savona, Italy
martina01.natali@edu.unife.it

Luca Brocca
Research Institute for Geo-
Hydrological Protection, National
Research Council
Perugia, Italy
luca.brocca@irpi.cnr.it

Sara Modanesi
Research Institute for Geo-
Hydrological Protection, National
Research Council
Perugia, Italy
sara.modanesi@irpi.cnr.it

Gabriëlle J. M. De Lannoy
Dept. of Earth and Environmental
Sciences, KU Leuven,
Heverlee, Belgium
gabrielle.delannoy@kuleuven.be

Christian Massari
Research Institute for Geo-
Hydrological Protection, National
Research Council
Perugia, Italy
christian.massari@irpi.cnr.it

Fabio Mantovani
Dept. of Physics and Earth Sciences,
University of Ferrara,
INFN Ferrara section,
Ferrara, Italy
mantovani@fe.infn.it

Abstract—This study presents a simple framework to calibrate a soil water balance model (SWB) with Sentinel 1 backscatter observations. The SWB is coupled with a Water Cloud Model (WCM) able to simulate backscatter from soil moisture and NDVI. The combined model, namely SWB(WCM), is calibrated by maximizing the Kling-Gupta Efficiency (KGE) between simulated backscattering values and observations from Sentinel-1. The procedure is carried out over data collected during a field campaign in 2017 at an experimental site in Budrio (BO), Italy, cultivated with tomato. The calibration scheme involves 7 parameters and presents good results in terms of backscatter calibration (KGE = 0.69). In order to evaluate the overall performance of the model, SM estimates from the SWB model are compared with *in-situ* SM measurements from a Proximal Gamma Ray Station (PGRS), showing promising results (KGE = 0.58) in the estimation of soil moisture, without requiring any *in-situ* soil moisture measurements for calibration.

Keywords—WCM, soil water balance, soil moisture, Sentinel-1

I. INTRODUCTION

Soil moisture (SM), namely the amount of water that is present in the soil in any form, is a key variable in irrigation and precision agriculture [1].

In the context of a changing climate and growing demand for water, accurately estimating SM becomes of vital importance for improving crop production, reduce crop failure and optimize irrigation applications. However, measuring SM over large agricultural areas with a sufficiently dense temporal resolution requires labor-intensive and costly field campaigns. Models are a viable alternative to overcome this difficulty, but they can be subjected to uncertainty in model parameters and forcing [2] and simplified assumptions on irrigation modelling [3,4]

New high resolution microwave remote sensing observations like those from Sentinel-1 (European Space Agency (ESA), Copernicus Missions) are on the other hand useful for monitoring soil moisture over irrigated fields as they contain realistic soil moisture spatiotemporal dynamics induced by irrigation and thus can be used to improve soil moisture estimates by models.

In recent years, there has been an increasing interest in improving SM estimates through the assimilation in land surface models of remote sensing observations such as radar backscattering coefficient (σ^0) observations [5,6]. σ^0 can be related to SM by modeling the dielectric behavior of the soil-water system and the vegetation canopy that covers it by means of radiative transfer models (RTM) [7], such as the Water Cloud Model (WCM, Attema and Ulaby, 1978) [8]. The latter is a forward, semi-empirical model which simulates σ^0 values as a function of *in-situ* SM data and vegetation indices (e.g., Normalized Difference Vegetation Index, NDVI) as inputs [9,10].

In this study, we present an alternative approach to classical sequential data assimilation that constrains a simple soil water balance model (SWB) coupled with WCM, i.e., SWB(WCM), with Sentinel 1 backscatter observations using calibration. The approach that provides SM estimates at potentially 10 m x 10 m spatial resolution with a hourly frequency is then validated against *in situ* soil moisture obtained from a Proximal Gamma Ray Station (PGRS).

II. MATERIALS AND METHODS

A. Experimental site and *in-situ* setup

Both the WCM and SWB require *in-situ* input data such as weather data, soil characteristics, crop information and irrigation measurements, which were gathered during an agricultural campaign in the period 4 April – 2 November 2017 (T2017 hereafter, after [11]), on a 0.15 ha portion of a test field managed by Acqua Campus, a research center of the Emiliano-Romagnolo Canal (CER) irrigation district in Budrio, near Bologna, Italy, which is showed in Fig. 1. The soil at the experimental site is characterized by a loamy texture, with wilting point equal to $0.09 \pm 0.01 \text{ m}^3 \text{ m}^{-3}$ and field capacity to $0.32 \pm 0.01 \text{ m}^3 \text{ m}^{-3}$ [12]. During the campaign, the field was cultivated with tomato (*Solanum lycopersicum*) and was irrigated with a sprinkler irrigation system, in accordance with a schedule provided by the IRRINET decision support tool [13].

In-situ measurements to validate the model were collected from a Proximal Gamma-Ray Spectroscopy (PGRS) station, also referred to as γ station, equipped with a 1 L NaI(Tl)

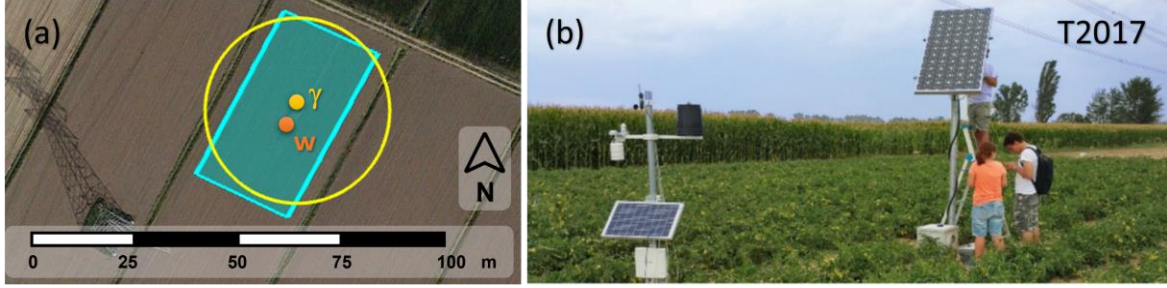


Fig. 1. After [8]. (a) The test field near Budrio, Bologna, with the positions of the PGRS station (γ) and agrometeorological station (w) and the area of interest (AoI) for σ^0 data (light-blue polygon). The yellow circle around the PGRS station represents the corresponding field of view (FOV) of a radius of about 25 m. (b) Picture of the two stations in 2017.

gamma-ray detector and a commercial agrometeorological station (MeteoSense 2.0, Netsens), both equipped with internet connection and powered by solar panels. The core of the PGRS station consisted of a 1 L sodium iodide (NaI(Tl)) gamma-ray spectrometer [14], placed atop a 2.25 m pole so that the field of view (FOV) of the PGRS station corresponded to a disk with a radius of approximately 25 m (Figure 2 of [15]), covering the entire field width, while approximately 60% of the signal was contributed by the first 6 cm of depth. In this study, the PGRS station was used to measure soil moisture (SM) by detecting gamma signals emitted in the decay of naturally present ^{40}K , which is typically homogeneously distributed in agricultural soil [12]. The measured SM from the PGRS station was used in this study to compare with the SM estimates obtained from SWB.

B. Remote sensing data

In this study, a total of 103 σ^0 observations from Sentinel-1 (S-1) were used for calibration. The S-1 data have high spatial resolution (10 m), making them suitable to study SM at the plot scale. Only co-polarized (VV) data are used, as previous research [16, 17] has shown that VV polarization is more sensitive to soil moisture and less sensitive to vegetation than cross-polarized (VH) data. σ^0 observations over the field come from three different relative orbits and are normalized to account for the different acquisition geometries. The procedure employs the whole historic series of observations on the test site from 2014 onwards and matches the pdfs of the observed values of each orbit to a reference one [18], which is chosen to be the one with an average incidence angle closest to 40° [19].

The model also employs as input a single vegetation descriptor, which is given by the Normalized Difference Vegetation Index (NDVI), calculated from Sentinel-2 (S-2). A total of 27 cloud-free observations have been used in this study, and values have been interpolated daily.

Data at 10 m spatial resolution from both satellite constellations were acquired from the Google Earth Engine (GEE) data collections and processed using Python scripts and the GEE Python API library *ee* (<https://github.com/google/earthengine-api/tree/master>). All the analyses were carried out by aggregating the data sets (in linear units) at the spatial scale of the test site.

III. MODEL

A. Soil water balance (SWB) model

SWB is an integral formula that returns the soil water content present in a certain soil layer at any given time [20], which is calculated as the sum of the water content that was

present at a previous time, precipitation and irrigation depth, minus evapotranspiration (ET) and deep percolation. This work employs a simplified soil water balance model developed by [21], in which the deep percolation term is parametrized as a cut of soil moisture at field capacity. The original model is suitable for estimating irrigation requirements, which instead in this specific case of model testing are used as input since they were collected during the T2017 campaign.

ET is calculated as the product of reference evapotranspiration, ET_0 , by the crop coefficient K_c and the crop stress coefficient K_s . Reference evapotranspiration ET_0 is calculated by using the hourly FAO Penman-Monteith method [20] and hourly weather measurements collected by the agrometeorological station. The crop coefficient K_c depends on the crop only (i.e. tomato) and varies with the stages of growth of the crop, having its minimum value $K_{c,ini} = 0.6$ at the initial and late stages and maximum value $K_{c,mid} = 1.2$ when tomatoes are fully developed. Its curve is built on reference values and standard lengths of the growing stages from Table 11 and 12 of [20]. Reference values should be corrected for the actual wetting frequency of the soil, soil texture and climate conditions, thus an empirical parameter $K_{c,0}$ is introduced in the model as a scaling factor of K_c to account for these adjustments. The stress coefficient K_s is a dimensionless transpiration reduction factor that depends on the soil water that is available to the plants. It ranges between 0 and 1, being 1 in the case of no water stress and optimal watering and management conditions and 0 when soil moisture reaches wilting point. K_s depends on the depletion fraction ρ , which in turn depends on the standard depletion fraction ρ_{st} and ET. ρ_{st} depends on the crop type and is fixed at its reference value for tomato crops, $\rho_{st} = 0.4 \text{ mm day}^{-1}$ from [20]. Since ρ is calculated for daily ET, hourly ET is multiplied by 24 when calculating ρ .

In the most general conditions, the volumetric soil water balance employed in this study is, at any given time i is (1):

$$SM_i = SM_{i-1} + (P_i + I_i - (ET_{0,i} * K_{c,i} * K_{c,0} * (SM_{i-1} - SM_w)) / (1 - \rho_{st} - 0.04(5 + ET_{0,i} * K_{c,i} * K_{c,0} * 24))(SM_{fc} - SM_w)) / \delta \quad (1)$$

where SM_i [m^3m^{-3}] is the volumetric soil moisture at time i , P [mm] is precipitation, I [mm] is irrigation depth, SM_w [m^3m^{-3}] is wilting point, SM_{fc} [m^3m^{-3}] is field capacity and δ is the depth of the soil layer investigated. δ is chosen to be

compatible with radar observation from S-1 and has an average value of about 30 mm. By construction, SM given by (1) can only take values between wilting point SM_w and field capacity SM_{fc} .

B. Water Cloud Model (WCM)

The Water Cloud Model (WCM) is a semi-empirical forward model employed to calculate the radar backscattering coefficient from vegetated areas, and corresponds to the zeroth order solution of the radiative transfer equation for single-scattering processes happening in a uniform and homogeneous vegetation layer placed above a soil layer. Backscattering is a quantity related to the scattering of radar signals, i.e. microwaves, and is a measure of the electromagnetic power received and re-emitted by a target. When the target is the Earth's surface, the scattering mechanisms that produce the reflected signal are surface and volume scattering from bare soil and vegetation, respectively. In the WCM, backscattering is given by the incoherent sum of the soil contribution, which depends linearly on soil moisture and is dumped by a two-way attenuation coefficient that accounts for the presence of vegetation, and the vegetation contribution, which depends on a bulk vegetation descriptor that follows the growth stages of the canopy. The WCM was first proposed in 1978 by Attema and Ulaby [8] as a generic model which can be parametrized in different ways and by employing different vegetation descriptors [7, 9]: The WCM which is used in this study takes as inputs soil moisture estimates calculated by SWB and employs a single bulk vegetation descriptor, to calculate σ (which stands for σ^0 in linear units) at any given time i [22], as expressed in (2):

$$\sigma = AV\cos\theta_i(1 - \exp(-2BV_i/\cos\theta_i)) + \exp(-2BV_i/\cos\theta_i)*\exp(C+D*SM_i) \quad (2)$$

where the first term represents the vegetation contribution σ_{veg} and the second term is given by the product of the exponential two-way attenuation coefficient, also known as γ^2 , and the soil contribution σ_{soil} . In (2) A, B, C, D are empirically fitted parameters and θ_i is the angle of incidence of the radar signal. The vegetation scheme involves a single bulk vegetation descriptor V_i , equal to NDVI, which has been shown in previous research to be suitable to use in WCM [16, 23, 24]. σ is expressed in linear units, as in the original formulation of Attema and Ulaby, and then converted to σ^0 [dB] to be compared with observations. The model was directly coupled with the SWB so as to provide a unique system of equations simulating backscatter.

C. Calibration strategy

The calibration strategy is based on the comparison between calculated backscattering values from SWB(WCM), σ_{sim}^0 hereafter, and actual S-1 observations, σ_{obs}^0 . More precisely, at each optimization step a timeseries of hourly SM values is produced over the whole study period based on the inputs of SWB and a tuple of guess values for the model parameters. Then, SM_i values are extracted corresponding to the same hour i in which the satellite observations took place, and are used as inputs in the WCM to produce a timeseries of σ_{sim}^0 values which are temporally matching with σ_{obs}^0 .

The model parameters are optimally chosen in order to maximize the Kling-Gupta Efficiency (KGE) [25] between simulated and observed values [5]. KGE is a commonly used metrics for evaluating the performance of hydrological models on timeseries, embedding three terms: Pearson's R,

bias and ratio of SD of the two populations. It takes a range of values between $-\infty$ and 1, the latter corresponding to a perfect accordance. The boundary conditions on the values of empirical parameters must be deduced by their mathematical role in the model, or at least their dependencies on physical observables. The parameters of the WCM depend mostly on the expected value of σ^0 , which for S-1 VV observations over bare and vegetated soil is in the range [-20, -5] dB [26], corresponding roughly to [0.1, 0.6] in linear scale. A and B are empirical scaling factors which values depend also on NDVI, that on well developed vegetation takes non negative values in the range [0, 1]. By following this line of reasoning and supposing an average angle of incidence of 40° , it is deduced that A and B must be small, non-negative quantities: A is taken in the range [0, 5], after [27], while B is taken in [0, 3]. C represents the radar backscatter from a perfectly dry soil and in principle should depend on soil texture and roughness only, and takes values in the range [-20, -5] dB, as previously stated. D relates to the sensitivity of the radar to variations in volumetric soil moisture and is in principle constant for any given soil texture profile [5]. Its range of values is chosen as [10, 100] dB m^3m^{-3} , after [27]. Concerning SWB, the only empirical parameter is $K_{c,0}$, i.e. the scaling factor of K_c : its expected mean value is 1, while its boundaries are reasonably chosen as 0 and 2 by considering the minimum and maximum values that K_c can reach in different conditions [20]. The other two variables which are calibrated in SWB are wilting point SM_w and field capacity SM_{fc} , which boundaries are determined at 3 SD from their central value from in situ measurements.

The calibration experiment on T2017 is performed by running the model multiple times (around 100) with the same hyperparameters' configuration of the optimizer, that is represented by a custom-made routine based on particle swarm optimization (<https://pyswarms.readthedocs.io/en/latest/>) [28]. This procedure produces distributions of values of the parameters, from which the medians (Q2) are taken as central values and the asymmetric uncertainties are given by the interquartile ranges, Q2-Q1 for left uncertainty and Q3-Q2 for right uncertainty.

IV. RESULTS AND DISCUSSION

The results on T2017 are presented in Table I. **L'origine riferimento non è stata trovata.** The central values of the parameters are then reinserted into the model to build the timeseries of σ_{sim}^0 and SM over the whole period of study (Fig. 2). The statistical measure of goodness of fit that is employed for σ^0 is the cost function itself, namely the KGE. The top panel of Fig. 2 shows the timeseries of σ^0 estimations VS their observations, along with the NDVI curve on the secondary axis. The good values of the coefficients $R = 0.69$ and of $KGE = 0.69$ indicate an overall good fitting. The low bias (bias = -0.04 dB) indicates that the model correctly reproduces the dynamics of σ^0 values without outliers.

TABLE I CALIBRATED MODEL PARAMETERS

Parameter	Median	Err
A [-]	0.347	[0.003, 0.012]
B [-]	0.692	[0.07, 0.03]
C [dB]	-14.5	[0.2, 0.1]
D [dB m^3m^{-3}]	29.2	[1.5, 1.7]
$K_{c,0}$ [-]	0.283	[0.012, 0.002]
SM_{fc} [m^3m^{-3}]	0.322	[0.014, 0.012]
SM_w [m^3m^{-3}]	0.098	[0.004, 0.004]

employed and of that the parameters' bounds are compatible

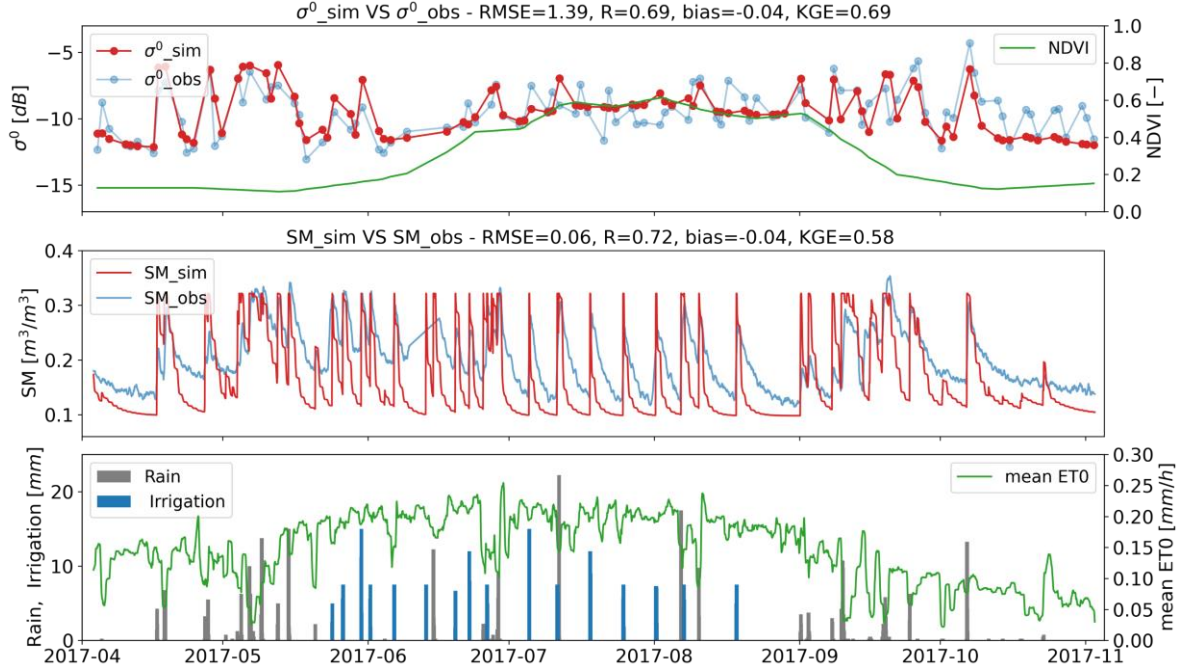


Fig. 2 Timeseries of σ^0 , soil moisture and inputs of the model during T2017. Top panel: observed (blue, with subscript “obs”) σ^0 VS simulated (red, subscript “sim”), along with NDVI values used as input in the WCM. The bias is measured in [dB]. Center panel: observed SM from the PGRS station VS simulated. The bias is measured in [mm]. The moving average of SM observations over 12 hours is presented for visualization reasons, along with the interpolation of eventual gaps. SM values are showed for comparison only and they do not enter in the calibration of the model anywhere. Bottom panel: timeseries of hourly irrigation, rain and hourly ET_0 , which represent the inputs of SWB. The plotted values of ET_0 correspond to the 24-hours moving average for visualization reasons.

The first part of the timeseries (i.e. during spring) is reproduced very precisely by the model. In this period no vegetation is present (described by a very low value of NDVI) and the soil contribution to σ^0 , σ^0_{soil} , which is dominated by SM dynamics, is dominant.

During the summer period, on the other hand, the dynamics of σ^0 with respect to SM variations is less clear and the modeling predictions present more discrepancies with the observations. This is due to i) higher values of NDVI, that decrease the value of the two-way attenuation coefficient γ^2 that multiplies the soil component of σ^0 in the factor $\gamma^2 \sigma^0_{soil}$, which is suppressed as a consequence; ii) the presence of a fully-grown vegetation canopy, which affects the observations themselves and make them less easy to model with such easy parametrization of the vegetation contribution to σ^0 . During summer, σ^0 follows closely the behavior of the NDVI curve, since the vegetation contribution is dominant. Some underlying dynamics due to SM variations is still visible since the value of parameter B is small (< 1): preliminary studies (not shown in this work) have showed that a value of B higher than 2 would lead to a complete suppression of σ^0_{soil} for such values of NDVI.

During fall, lower NDVI values lead to σ^0_{soil} being dominant again as during spring. A higher variability of observations is visible on the final part of the timeseries (second half of October 2017), which is not consistent with observed or modelled SM variability. Since σ^0 observations are normalized by their incidence angle and therefore cannot be affected by it, the phenomenon may be an indication of scattering effects that have not been considered in this study and cannot be explained by WCM.

Concerning SM estimates, the goodness of the fit ($KGE > 0.6$) is an indication of the reliability of the SWB model

with their true in-situ values. The most obvious discrepancy between simulated and measured values is given by the slope of the decrease in soil moisture after a wetting event, which corresponds to the rate at which the soil dries out. This term depends on both the ET rate and the soil layer depth, encompassing all variables of SWB, namely SM_{fc} , SM_w , $K_{c,0}$, ρ_{st} , δ . The parameters that are dominant in the process are δ , ρ_{st} , $K_{c,0}$, since SM_{fc} , SM_w only regulates the range of the dynamics of SM (i.e. the distance between the maximum and minimum values that can be reached). In particular, the depth of the soil layer is fixed at 3 cm, while the depth of investigation of the PGRS station, on the other hand, is about 6 cm. Since a shallower soil layer dries out faster than a deeper one, the discrepancy between the slopes of the SM curves may be due to the different soil layers that are investigated by the in-situ PGRS station and S-1.

V. CONCLUSIONS

This work presents a simple framework to calibrate a SWB coupled with a Water Cloud Model (WCM), namely SWB(WCM), for calculating soil moisture over irrigated fields. The model presents is able to provide soil moisture at field scale (30 m x 50 m) with temporal resolution of 1h. The model presents good results in reproducing both backscattering ($KGE = 0.69$) and soil moisture ($KGE = 0.58$) dynamics over an agricultural field in both bare and vegetated conditions. The calibration of this model is only based on remote sensing observations, which are free to use and easy to retrieve and doesn't require any in-situ soil moisture measurement. The main current limitation of the proposed approach is the depth of the simulated soil moisture. Future works will indeed investigate different model structures and calibration options to provide information also on the root zone soil and irrigation applications.

ACKNOWLEDGMENT

"We would like to acknowledge the support of the ESA projects 4D MED Hydrology (Contract no. ESA 4000136272/21/I-5 EF) and DTE Hydrology Evolution (Contract no. ESA 4 4000136272/21/I-EF - CCN N. 1)".

REFERENCES

- [1] Lei F, Crow WT, Kustas WP, et al. "Data Assimilation of High-Resolution Thermal and Radar Remote Sensing Retrievals for Soil Moisture Monitoring in a Drip-Irrigated Vineyard", *Remote Sensing of Environment*. 2020 Mar;239. DOI: 10.1016/j.rse.2019.111622. PMID: 32095027; PMCID: PMC7038819.
- [2] Renard, B., Kavetski, D., Kuczera, G., Thyer, M., & Franks, S. W., "Understanding predictive uncertainty in hydrologic modeling: The challenge of identifying input and structural errors", *Water Resources Research*, 46(5), 2010. <https://doi.org/10.1029/2009WR008328>
- [3] McDermid, S., Nocco, M., Lawston-Parker, P., Keune, J., Pokhrel, Y., Jain, M., Jägermeyr, J., Brocca, L., Massari, C., Jones, A. D., Vahmani, P., Thiery, W., Yao, Y., Bell, A., Chen, L., Dorigo, W., Hanasaki, N., Jasechko, S., Lo, M.-H., ... Yokohata, T., "Irrigation in the Earth system", *Nature Reviews Earth & Environment*, 1–19, 2023. <https://doi.org/10.1038/s43017-023-00438-5>
- [4] Massari, C., Modanesi, S., Dari, J., Gruber, A., De Lannoy, G. J. M., Giroto, M., Quintana-Seguí, P., Le Page, M., Jarlan, L., Zribi, M., Ouadi, N., Vreugdenhil, M., Zappa, L., Dorigo, W., Wagner, W., Brombacher, J., Pelgrum, H., Jaquet, P., Freeman, V., ... Brocca, L., "A review of irrigation information retrievals from space and their utility for users", *Remote Sensing*, 13(20), 2023. <https://doi.org/10.3390/rs13204112>
- [5] Lievens, H., et al., "Assimilation of global radar backscatter and radiometer brightness temperature observations to improve soil moisture and land evaporation estimates", *Remote Sensing of Environment*, 2017. 189: p. 194-210.
- [6] Modanesi, S., et al., "Optimizing a backscatter forward operator using Sentinel-1 data over irrigated land", *Hydrology and Earth System Sciences*, 2021. 25(12): p. 6283-6307.
- [7] Weiß, T., et al., "Evaluation of Different Radiative Transfer Models for Microwave Backscatter Estimation of Wheat Fields", *Remote Sensing*, 2020. 12(18).
- [8] Attema, E.P.W. and F.T. Ulaby, "Vegetation modeled as a water cloud", *Radio Science*, 1978. 13(2): p. 357-364.
- [9] A.J. Graham and R. Harris, "Extracting biophysical parameters from remotely sensed radar data: a review of the water cloud model", *Progress in Physical Geography*, 2003. 27: p. 217-229.
- [10] Ma, C., et al., "Global Sensitivity Analysis of a Water Cloud Model toward Soil Moisture Retrieval over Vegetated Agricultural Fields", *Remote Sensing*, 2021. 13(19).
- [11] Serafini, A., et al., "Proximal Gamma-Ray Spectroscopy: An Effective Tool to Discern Rain from Irrigation", *Remote Sensing*, 2021. 13(20).
- [12] Strati, V., et al., "Modelling Soil Water Content in a Tomato Field: Proximal Gamma Ray Spectroscopy and Soil-Crop System Models", *Agriculture*, 2018. 8(4): p. 60.
- [13] Munaretto, S. and A. Battilani, "Irrigation water governance in practice: the case of the Canale Emiliano Romagnolo district, Italy", *Water Policy*, 2014. 16(3): p. 578-594.
- [14] Baldoncini, M., et al., "Biomass water content effect in soil water content assessment via proximal gamma-ray spectroscopy", *Geoderma*, 2019. 335: p. 69-77.
- [15] Baldoncini, M., et al., "Investigating the potentialities of Monte Carlo simulation for assessing soil water content via proximal gamma-ray spectroscopy", *J Environ Radioact*, 2018. 192: p. 105-116.
- [16] Baghdadi, N., et al., "Calibration of the Water Cloud Model at C-Band for Winter Crop Fields and Grasslands", *Remote Sensing*, 2017. 9(9).
- [17] Vreugdenhil, M., et al., "Sensitivity of Sentinel-1 Backscatter to Vegetation Dynamics: An Austrian Case Study", *Remote Sensing*, 2018. 10(9).
- [18] Mladenova, I.E., et al., "Incidence Angle Normalization of Radar Backscatter Data", *IEEE Transactions on Geoscience and Remote Sensing*, 2013. 51(3): p. 1791-1804.
- [19] Wagner, W., et al., "Data Retrieval in Earth Observation - Course Material", Vienna University of Technology, Department of Geodesy and Geoinformation, 2019.
- [20] Allen, R.G., et al., "Crop evapotranspiration-Guidelines for computing crop water requirements - FAO Irrigation and drainage paper 56", FAO, Rome, 1998. 300(9): p. D05109.
- [21] Rolle, M., S. Tamea, and P. Claps, "ERA5-based global assessment of irrigation requirement and validation", *PLoS One*, 2021. 16(4): p. e0250979.
- [22] Prévot, L., I. Champion, and G. Guyot, "Estimating Surface Soil Moisture and Leaf Area Index of a Wheat Canopy Using a Dual-Frequency (C and X Bands) Scatterometer", 1993.
- [23] Dabrowska-Zielinska, K., et al., "Soil Moisture in the Biebrza Wetlands Retrieved from Sentinel-1 Imagery". *Remote Sensing*, 2018. 10(12).
- [24] Li, J. and S. Wang, "Using SAR-Derived Vegetation Descriptors in a Water Cloud Model to Improve Soil Moisture Retrieval", *Remote Sensing*, 2018. 10(9).
- [25] Gupta, H.V., et al., "Decomposition of the mean squared error and NSE performance criteria: Implications for improving hydrological modelling", *Journal of Hydrology*, 2009. 377(1-2): p. 80-91.
- [26] Bauer-Marschallinger, B., et al., "Toward Global Soil Moisture Monitoring With Sentinel-1: Harnessing Assets and Overcoming Obstacles", *IEEE Transactions on Geoscience and Remote Sensing*, 2019. 57(1): p. 520-539.
- [27] Rains, D., et al., "Sentinel-1 Backscatter Assimilation Using Support Vector Regression or the Water Cloud Model at European Soil Moisture Sites", *IEEE Geoscience and Remote Sensing Letters*, 2022. 19: p. 1-5.
- [28] Kennedy, J. and Eberhart, R.: "Particle swarm optimization", *Proceedings of ICNN'95 – International Conference on Neural Networks*, Perth, WA, Australia, pp. 1942–1948, vol. 4, 1995. <https://doi.org/10.1109/ICNN.1995.488968>, 1995.